Role of Glassy Bridges on the Mechanics of Filled Rubbers under Pressure

Jonathan Champagne, S. Cantournet, Davide Colombo, S. Jamonneau, K. Le Gorju, F. Lequeux, H. Montes

Role of glassy bridges on the mechanics of filled rubbers under pressure

J. Champagne,[*,†,‡] S. Cantournet,[†] D. Colombo,[†] S. Jamonneau,[¶] K. Le Gorju,[¶] F. Lequeux,[‡] and H. Montes[‡]

PSL University, Mines ParisTech, Centre des Matériaux, CNRS 7633 BP 87, F-91003 Evry Cedex, France, PSL University, ESPCI Paris, Sciences et Ingénierie de la Matière Molle, Paris Cedex 5, France, and Hutchinson SA, Research and Innovation Centre, Châlette-sur-Loing, France

E-mail: jonathan.champagne@mines–paristech.fr

---

[*]To whom correspondence should be addressed
[†]Mines ParisTech
[‡]ESPCI
[¶]Hutchinson

1

Abstract

In this study, we address the question of the equivalent role of the pressure and temperature on the mechanical properties of highly filled elastomers. It is well known that in polymer matrixes, the equivalence of temperature and pressure results from free volume variations. Our measurements performed on phenylated polydimethylsiloxane (PDMS) chains filled with silica particles show that a temperature-pressure superposition property is still observed in both linear and nonlinear regimes in these systems. However, the temperature-pressure equivalence involves coefficients that are two orders of magnitude larger than those in non-reinforced matrixes. We suggest that the mechanical response of the filled elastomers is controlled by the shape of the rigid network made by fillers that are connected by rigid polymer bridges. In this frame, we provide quantitative evidence that the macroscopic behavior of reinforced elastomers is controlled by the variation in the degree of the confinement of polymer chains between particle surfaces.

1. Introduction

The addition of fillers - spherical particles of carbon black or silica - into a polymer matrix brings an outstanding enhancement in the mechanical properties.[1] Not only does the stiffness of the material increase but also the hysteresis during cyclic solicitations,[2] fatigue strength and abrasion resistance increase. Hence, filled rubbers have enabled many niche solutions for the industry.[3] Although the addition of fillers results in complex thermomechanical behavior, the polymer matrix can be satisfactorily described. First, the viscoelastic response of filled elastomers is different since the classical entropic behavior, i.e., the growth of the modulus proportional to the temperature, progressively disappears as the filler proportion increases.[4] Second, the addition of fillers introduces significant strain amplitude nonlinearities, often referred to as the Mullins effect[5] and Payne effect.[6] The specific mechanical features observed on the filled rubbers are commonly explained by considering a rigid network formed by fillers

within a polymer matrix and its modification with the temperature and strain amplitude.[7–10] According to this scenario, the variation in the stiffness of the sample is thus controlled by the connectivity of the network that involves polymer chains close to the particle surface. For instance, Maier and Goritz[11] underlined the influence of the desorption/absorption mechanism for polymer chains near the particle surface. Moreover, the dynamics of the polymer chains close to the particle surface appears to be slowed down by confinement.[12–17] Because the mechanical response of these chains is stiffer than that in the bulk, the confined polymer chains form rigid polymer bridges connecting the particles within the sample.

If the temperature and strain amplitude significantly contribute to the mechanical properties of filled rubbers, then the pressure is also known to influence the mechanical response. In most industrial applications, parts composed of filled rubbers are preloaded in compression. If their shape has a large aspect ratio, then the compression force results in a significant hydrostatic pressure. Studies performed on a pure polymer matrix[18–21] have reported a stiffening of the mechanical response due to a decrease in the free volume fraction[22] in the sample. Merabia and Long[23] even pointed out that the distribution of the free volume within the system is at the origin of the observed dynamics. Thus, the increasing pressure shifts the glass transition temperature toward a high temperature according to the relation:

$$\frac{\partial T_g}{\partial p} = \alpha \tag{1}$$

where α can be obtained through pressure-volume-temperature measurements,[24–27] stress relaxation modulus experiments,[19] and Young's modulus[18] or dielectric properties[20] measurements. More recently, the pressure effect was investigated through shear-compression tests.[21] Unanimously, regardless of the experimental technique, the results have shown that α varies from 0.1 to 0.6 K/MPa depending on the polymer matrix as classified in the standard pressure-volume-temperature data for polymers.[27] In this frame, temperature-pressure superposition is obtained for the relaxation of the modulus of the polymer matrix.

Although the pressure dependence of the mechanical response of a pure polymer matrix has been widely investigated for the last 70 years, there have been only a few studies devoted to the response of filled rubbers under pressure. Fillers and Tschoegl[19] observed the time-temperature-pressure superposition in the case of elastomers filled with less than 8 % in volume of carbon black particles; their results were explained by the variation in the free volume of the samples. However, these authors did not consider the effect of pressure on the filler network.

In this work, we compare the effect of pressure and temperature on the mechanical response of a filled rubber that contains a 27 % silica nanoparticle volume. The equivalence between the temperature and pressure on the linear and nonlinear responses is analyzed by taking into account the modifications involved by pressure on the rigid network composed of particles connected by confined polymer chains. In addition, the variation in the free volume fraction reported for the bulk polymer matrix is also taken into account. With this objective, we analyzed the effect of pressure on the mechanical response of polymer chains confined between particle surfaces. Our approach is based on the understanding of the dynamics of confined polymers built over the last 20 years from experimental measurements, theories and simulations. Vogt,[28] and references therein, has provided a good review on the significant impact of the confinement of amorphous polymers in nanoscale dimensions on their mechanical properties. Many authors[29–32] have revealed that the glass transition temperature T_g of thin polymer films strongly interacting with a solid substrate increases with decreasing film thickness. Similar effects of the confinement on the dynamics of polymer chains located between neighboring particles are thus expected in filled elastomers. Many studies performed on filled rubbers have shown the existence of a mobility gradient for polymer chains located between neighboring particles.[12–17] According to the picture developed from the behavior measured on confined thin films, the slowing down of the polymer dynamics observed in filled elastomers can be described assuming a glass transition gradient for polymer chains confined between neighboring particles. A local glass transition temperature $T_g(z)$ can be

defined, which depends on the distance z of polymer chains from the particle surface. In this framework, polymer chains with a local $T_g(z)$ higher than the temperature of experiment T will behave similar to glassy polymers. These chains will form a layer of glassy polymer that surrounds the particle surface (see Figure 1). Studies have shown that the thickness of this layer decreases with temperature.[4,33,34] If the glass transition temperature at the half distance between neighboring particles is higher than the temperature of the experiment, then fillers will thus be connected by rigid bridges made of a glassy-like polymer[34,35] (see Figure 1).
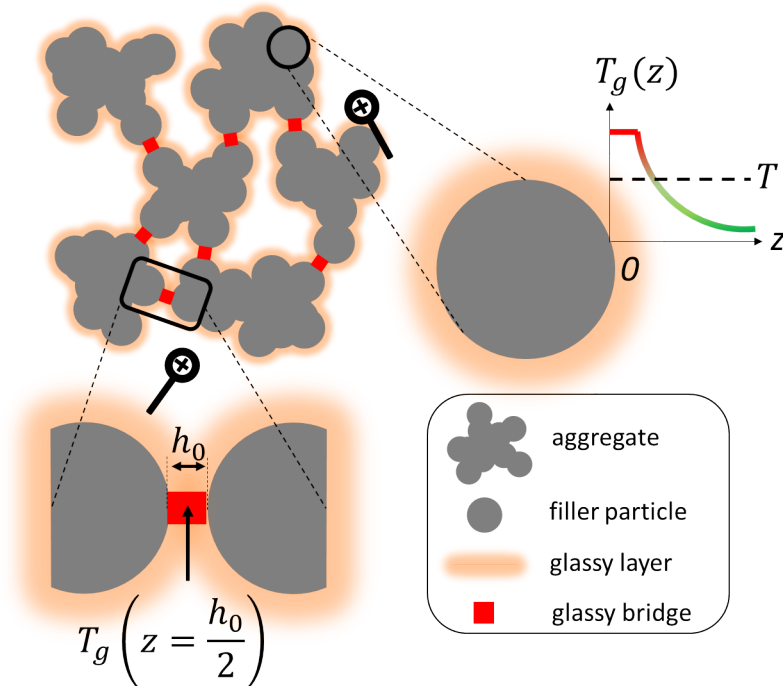

Figure 1: Schematic view of the glassy bridges in filled rubbers at T

These important physical phenomena have already been used by many authors to describe the mesoscale behavior of filled rubbers. Merabia et al.[36] developed a microscopic model by considering a volume fraction of randomly distributed filler in which the interaction between two neighboring particles is driven by two forces. A permanent contribution represents the polymer matrix contribution, and a larger nonpermanent contribution represents the glassy bridge contribution, which has a finite lifetime depending on the temperature. These

researchers have pointed out that strong reinforcement is obtained when glassy layers between fillers overlap. In another example, Froltsov et al.[37] investigated the rupture mechanisms in a glassy bridge through molecular dynamics simulations. These investigators observed the effects of the confinement, i.e., the glassy bridge length, and the temperature on the structure and mechanics during a rupture. In more recent studies, Sodhani and Reese[38] performed a finite element (FE) simulation of a nanocomposite microstructure composed of fillers within a polymer matrix. To incorporate the T_g gradient in the vicinity of the particles, these authors distinguished two polymer phases by their dynamical properties. In the first phase, chains were bound to the filler surfaces and were in their glassy state. The second phase corresponds to the chains in the rubber state. In this approach, the proportion of the two phases does not evolve with the temperature. Moreover, the micromechanical approaches described above do not account for the effect of pressure.

The paper is organized as follows. First, the material and the experimental conditions are described. Experiments under pressure are performed using poker chip geometry samples,[39–41] i.e., whose shape has a large aspect ratio in order to apply a large pressure to the material. We show that the pressure effect on filled rubbers is larger by approximately two orders of magnitude than the contribution associated with the variation in the free volume that is measured on the polymer matrix. Second, we discuss the pressure effect on the dynamics of the polymer chains located in glassy bridges. With this objective, we first assume that the stress is mostly sustained by the particle network connected by the confined polymer in the glassy state. We show that the local behavior is governed by two contributions at the glassy bridge scale: the confinement of polymer chains between particle surfaces and the variation in their free volume fraction. In this context, we show that the variation in the confinement degree controls the macroscopic response of the filled rubbers. Finally, we derive a new temperature-pressure superposition law for filled rubbers that is validated by our experiments performed under varying pressure and temperature.

6

2. Experiments

2.1. Material

The experiments are performed on a poly(dimethylsiloxane-codiphenylsiloxane) matrix highly filled with silica nanoparticles. Based on nuclear magnetic resonance (NMR) measurements, the molar proportion of diphenylsiloxane groups is estimated at 5 %. The weight fraction of fillers is found to equal 50 % from thermogravimetric analysis. Assuming the following densities, 2.65 g/cm^3 for the silica and 0.965 g/cm^3 for the polymer matrix, the volume fraction is 27 %. From differential scanning calorimetry (DSC), the bulk glass transition temperature T_g^∞ is found to be approximately 158 K for a temperature rate of $+20$ K/min.

2.2. Description of the experimental tests

Cyclic shear tests are carried out under a controlled temperature ranging from 213 K to 303 K in a climatic chamber (Thermcraft incorporated) cooled by injecting nitrogen. Mechanical measurements are performed using the following geometries (see Figure 2).

- A double-shearing geometry is used to characterize the material mechanical behavior at zero pressure (atmospheric pressure). Two rubber pieces, each of them 4 mm thick are covalently bonded to inox plates with a thickness of 2 mm. Mechanical measurements are performed with a dynamic mechanical thermal analysis (DMTA) viscoanalyser (VA4000 from Metravib) applying a cyclic shear strain $\gamma(t) = \Delta\gamma.sin(2\pi ft)$.

- A poker chip geometry with a large aspect ratio is used to measure the mechanical response of our filled elastomer under pressure. A 2.5 mm thick rubber disc is covalently bonded between two cylinders made of alloy. The diameter of the disc was chosen to be 25 mm. The aspect ratio a, which is defined as the ratio between the diameter and thickness of the disc, is equal to 10. We will show later that such an aspect ratio ensures a parabolic hydrostatic pressure field within the sample. During an experiment, the

7

filled rubber undergoes both a static compression force F_c and a cyclic shear strain $\gamma(t) = \Delta\gamma.sin(2\pi ft)$. In our study, F_c is varied from 400 N to 1500 N. For each static compression force, the amplitude of the cyclic shear strain $\Delta\gamma$ is varied from 2 % to 20 %. Figure 3 presents the experimental setup designed to be adapted in an Instron 8801 testing machine ($\pm 50\ kN, \pm 75\ mm$). For symmetry reasons, two poker chips are loaded simultaneously. The hydraulic cylinder displacement, in the horizontal direction (in Figure 3), provides the cyclic shear strain. To limit heat build-up due to the thermomechanical coupling,[42] the frequency f is kept at 1 Hz. Two calibrated springs (HPC R204608, external diameter: 32 mm, internal diameter: 16 mm, free length: 51 mm) of constant stiffness (134 N/mm) are used across the entire experimental temperature range. Thus, the compression of these two axial springs ensures a static compression force, independent of the temperature, as the thermal dilation of the setup does not significantly modify the force exerted by the springs.
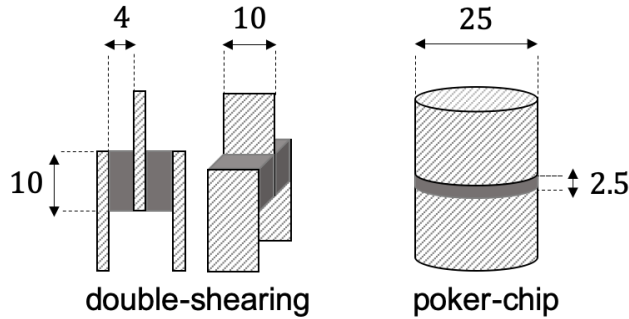

Figure 2: Samples geometries. Dimensions are given in mm

Measurements reported in this work have been performed by applying the 3 stage protocol that is presented in Figure 4:

- Stage 1: The two springs are squeezed to ensure the specified static compression force. Then, the climatic chamber is sealed and cooled at a temperature rate of approximately $-3\ K/min$. An isotherm of 60 min at the temperature of the measurements is applied such that the setup and the sample reached the equilibrium temperature
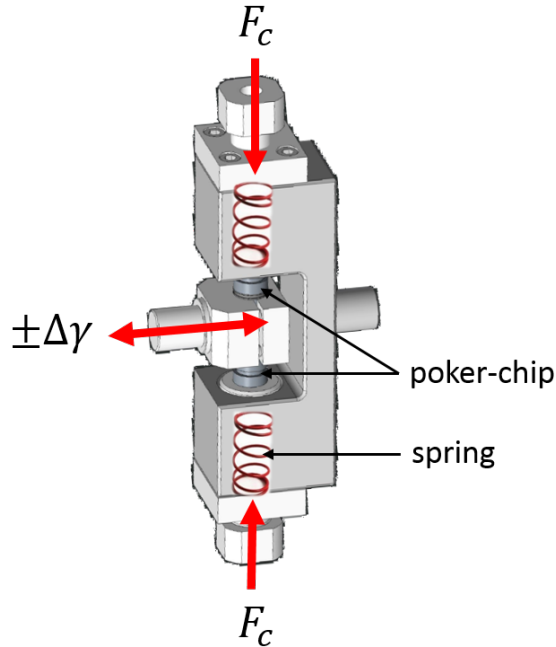
8

Figure 3: Overview of the experimental setup used for the shear-compression tests

at the beginning of the mechanical solicitation. Moreover, the sample temperature is checked so that it does not evolve during the two following stages of our experimental procedure.

- Stage 2: As shown by Chazeau et al.,[43] to measure the stabilized mechanical response of our filled elastomers, the Mullins effect[5] needs to be erased. Thus, in stage 2, an increasing strain sweep is applied that is followed by a second decreasing sweep. The amplitude of the strain ranges between 2 % and 20 %. For each shear strain amplitude value, 50 cycles are applied to the sample. Figure 4 also illustrates the stress-strain relation obtained within these two successive strain sweeps. The Mullins effect results in a change in the mechanical response measured at a given strain amplitude between the first increasing strain sweep and the next decreasing strain sweep. As expected, at the end of stage 2, the Mullins effect is erased from the mechanical behavior of our samples.

- Stage 3: A final increasing strain sweep (ranging from 2 % to 20 %) is applied. As

9

shown in Figure 4, the stress-strain relation is perfectly stabilized (green thick curves) and is similar to the decreasing strain sweep of stage 2. Therefore, all the following experimental results will be based on the measurements performed in this final stage and will correspond to the stabilized mechanical behavior of our samples. For each shear strain amplitude, 50 cycles are applied to the sample. We verified that the stress-strain responses measured during the last 10 cycles are similar. The values of the complex shear modulus are determined from the average response estimated from these last 10 cycles.
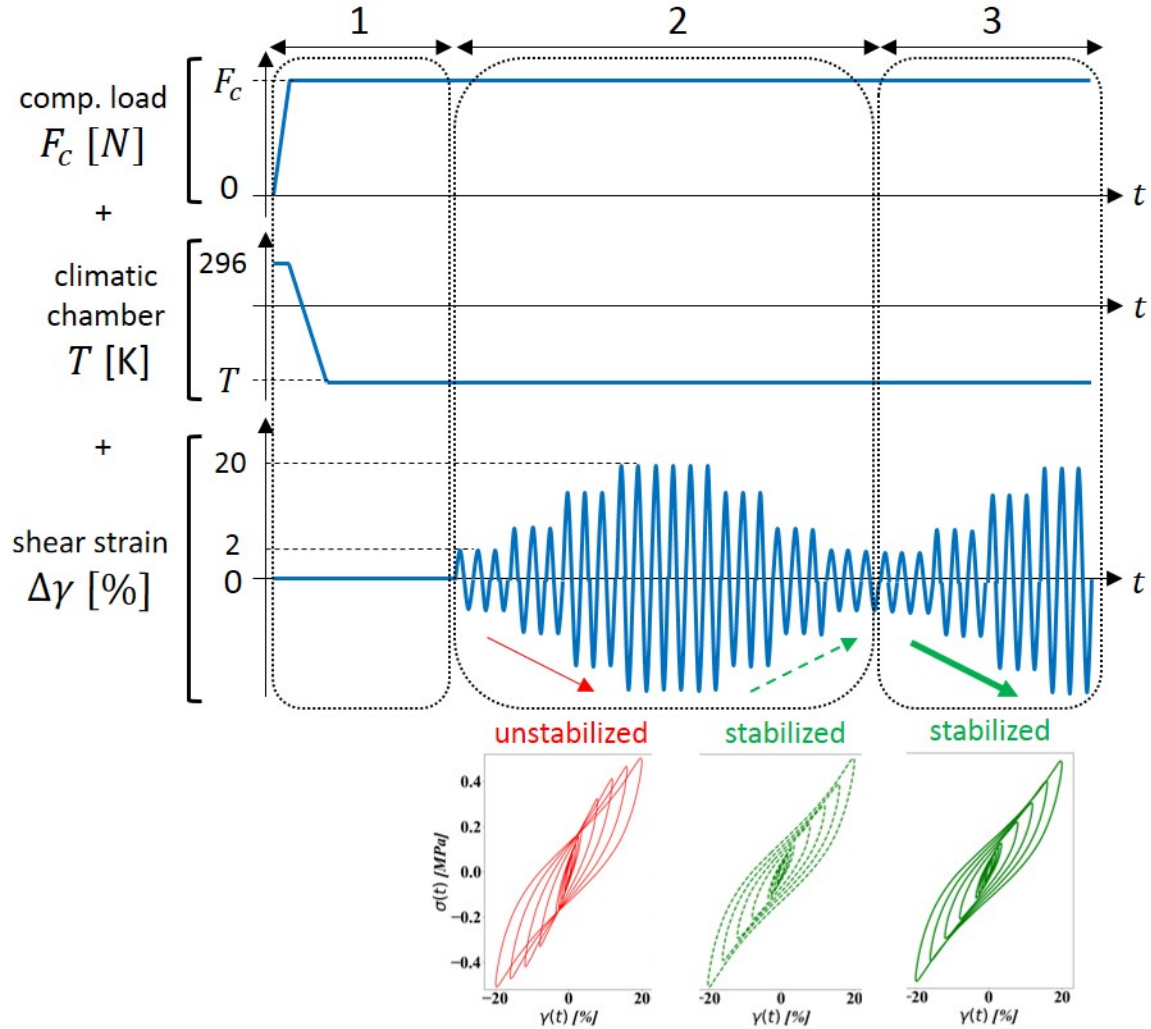

Figure 4: Experimental protocol: static compression force, temperature and shear strain amplitude evolutions

Measurements with the double-shearing geometry are performed by applying the same strain sweep history but without an applied compression force applied ($F_c = 0\ N$).

2.3. Experimental results

2.3.1. Shear strain amplitude, temperature and static compression force influences

Figure 5 presents the variation in the shear storage modulus G' as a function of the shear strain amplitude for a set of temperature and compression force conditions (T, F_c). In the absence of the static compression force (left chart), the dependence on the strain amplitude and temperature of our samples follows the general trends observed in the filled rubbers. Indeed, as reported on many filled elastomers for temperatures larger than $T_g^\infty + 50\ K$, the shear storage modulus of our system decreases with temperature.[4] We also observe a decrease in its value with increasing shear strain amplitude (Payne effect[6]). All these features are still observed if a static compression force ($F_c \neq 0\ N$) is applied to the sample (chart at the center of Figure 5). As shown on the right chart (Figure 5), applying a static compression force increases the shear storage modulus of our system measured at a given temperature and strain amplitude.

We must now precise the pressure distribution within the poker chip geometry. The parabolic pressure profile inside a compressed film is a finding of the lubrication theory by Reynolds,[44] later reconsidered in the context of bounded rubber layers by Rocard, Gent et al.,[45–47] Lindsey et al.[39,48] and many other authors.[40,41,49–51] We have also investigated the pressure distribution within the poker chip sample with the aid of a FE analysis described in the Appendix 6.2. As expected, applying a static compression force on a quasi-incompressible matrix in the poker chip geometry used in this work is equivalent to applying a hydrostatic pressure to the sample. Hence, the macroscopic mechanical response of the poker chip sample
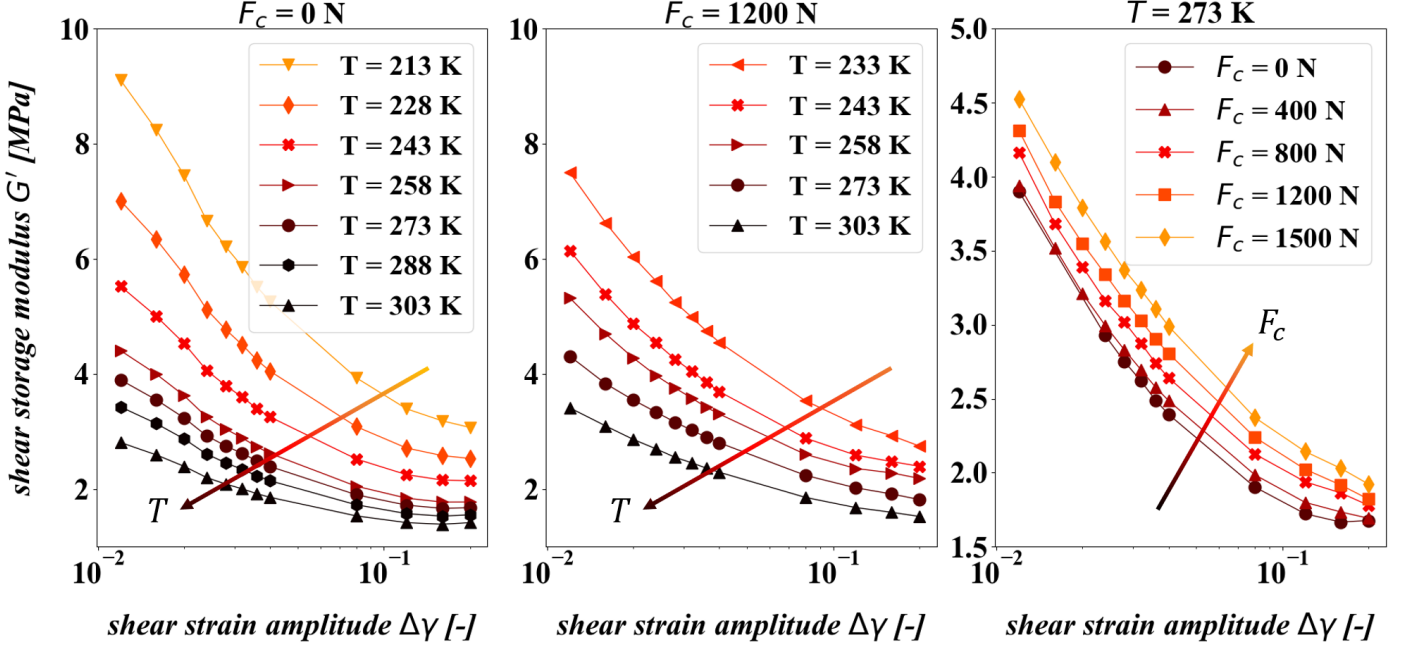
Figure 5: (left) and (center) Experimental measurements of the shear storage modulus as a function of the shear strain amplitude at various temperatures: (left) $F_c = 0$ N and (center) $F_c = 1200$ N. (right) Experimental measurements of the shear storage modulus at $T = 273$ K as a function of the shear strain amplitude under various static compression force conditions

can be assumed to be the one observed at an average hydrostatic pressure p given by

$$p = \frac{F_c}{S} \tag{2}$$

where S is the sample disc surface. Therefore, in the following, we will convert the compression force F_c into an average hydrostatic pressure p.

2.3.2. Temperature-pressure superposition

The experiments performed on our filled rubbers show that the temperature and pressure play antagonist roles with respect to their shear mechanical behavior. This feature raises the question of the equivalence between the pressure and temperature. Clearly, Figure 6 shows that equivalent mechanical responses are measured for several experimental conditions

(T, p). Such a stress-strain curve superposition highlights the existence of a temperature-pressure equivalence, which is observed in both linear and nonlinear regimes. According to the complete set of results, we find that an increase in the pressure of 1 MPa is equivalent to a temperature change of approximately -15 K. Thus, the order of magnitude of the pressure effect is approximately 15 K/MPa in our filled rubber which is approximately two orders of magnitude larger than that measured in pure rubbers.
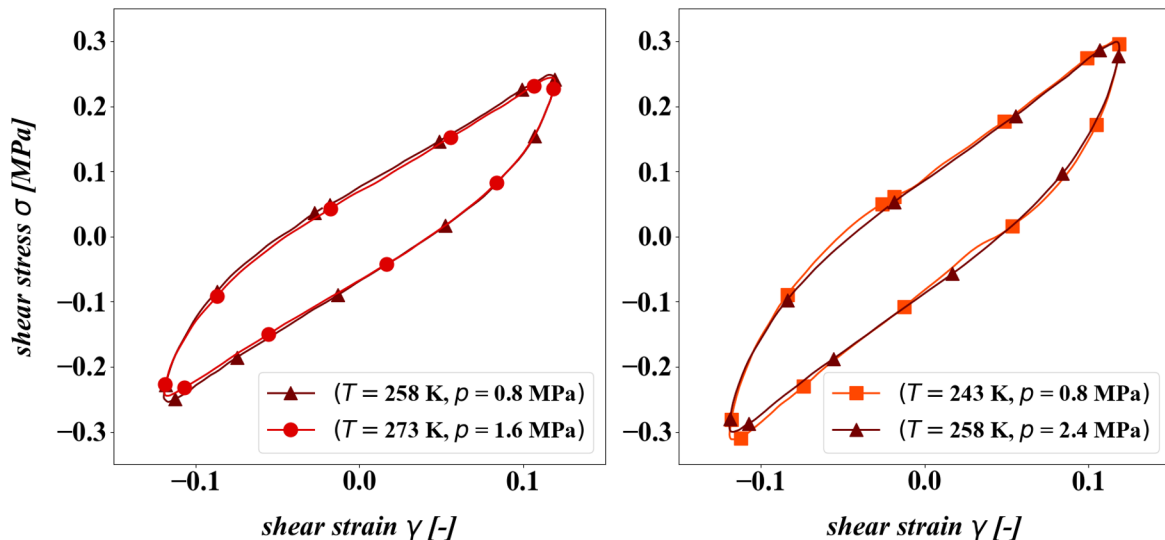

Figure 6: Examples of the stress-strain curve superposition measured at a given shear strain amplitude $\Delta\gamma = 12$ %

In the next section, we will analyze our experimental results assuming that the mechanical response of our system is essentially driven by the behavior of the glassy bridge network.

3. Pressure effect on the glassy bridges

3.1. The concept of glassy bridges

In this work, we assume that the mechanical behavior of filled rubbers is driven at the mesoscale by a rigid filler network connected by confined polymer chains in the glassy state. In our approach, each glassy bridge is described by a three-dimensional (3D) orientation and a length h_0, which corresponds to the confinement distance, i.e., the distance between the

neighboring particle surfaces at rest (see Figure 1). Assuming a T_g gradient for polymer chains in the vicinity of the particle surface, as proposed by Colombo et al.,[35] each glassy bridge has its own mechanical response depending on its length. As a result, the shape of the rigid network depends on the temperature. Indeed, the particles will be connected by a glassy bridge only if the temperature of the experiment is lower than the local glass transition temperature at the half length of the bridge ($z = h_0/2$ in Figure 1). Accordingly, the model of Long and Lequeux[52] can be expressed by

$$T_g\left(z = \frac{h_0}{2}\right) = T_g^\infty\left(1 + \frac{4\delta}{h_0}\right) \tag{3}$$

where T_g^∞ is the bulk glass transition temperature of the polymer matrix and $\delta \sim 1\ nm$ fixes the range of the T_g gradient measured by some authors.[53–56]

Thus, the key point of our model is the value of the glass transition temperature at the half distance $T_g(z = h_0/2)$ between neighboring particles compared to the temperature of the experiment. Because the value of the modulus of polymer chains abruptly decreases above T_g, we assume that the mechanical response of a polymer bridge is similar to that of polymer chains located at the middle of the bridge.[35] In this frame, we can compare the effect of temperature and pressure on the mechanical response of filled rubbers.

3.2. Pressure effects on the filled rubber

When pressure is applied to such a system, three contributions are expected. First, in accordance with the free volume theory,[22] the bulk glass transition temperature is shifted as the fraction of the free volume within the matrix decreases. According to Eq. 1, that contribution will induce a shift in the bulk glass transition of approximately $0.3\ K/MPa$ for a silicone matrix.[18,27] Second, if we assume that most of the stress is sustained by the filler network, then the local pressure within the glassy bridges is amplified due to geometrical considerations (i.e., a significant ratio between the particle diameter and the bridge length).

Using the analytical expression given by Cho and Gent,[57] we verify that this geometrical amplification of pressure within the glassy bridge is negligible in terms of the shift in the glass transition temperature with respect to the free volume theory (approximately $0.6\ K/MPa$ for a bridge length $h_0 = 3\ nm$ and a particle diameter $2R_p = 10\ nm$). Simultaneously, some aggregates appear closer to each other because of the pressure felt by the filler network. This modification of the shape of the filler network changes the degree of the confinement of the polymer chains between aggregates. According to Eq. 3, this behavior results in a change in the local glass transition within the glassy bridges. Because the effect of pressure that we macroscopically measured on our filled elastomers is approximately two orders of magnitude larger than that observed on pure rubbers, we deduce that the effect of pressure on the confinement degree is the main mechanism that drives the mechanical response of our filled rubbers under pressure. In addition, according to the literature, we will assume that the macroscopic stress is mainly sustained by the network in our highly filled rubber.

3.3. Amount of force sustained by the glassy bridges

As described in the introduction (see Eq. 3), the local mechanical behavior of the glassy bridge is governed by the local confinement, i.e., the distance between neighboring particle surfaces. We can estimate the amount of force sustained by each glassy bridge.

Assuming that the stress is sustained by the particle network, the force passes from an aggregate to the another neighboring aggregate. In granular media, under uniaxial loading, the forces between grains are nearly isotropically distributed along all directions.[58] Thus, we will assume, by analogy, that this is also the case in our filled rubber. In the following, we will assume that there is also an isotropic distribution of forces in our rigid network, even if a uniaxial compression force is applied to the samples. Therefore, for the sake of simplicity, we have chosen the pressure as the relevant parameter to describe the mechanical response observed in our filled elastomer.

Due to the pressure felt by the network, the aggregates are coming closer, and the axial

force is transmitted through the neighboring aggregates. In Figure 7, the force f_z sustained by the aggregate is the same as that sustained by the glassy bridge. We can deduce f_z from the pressure applied on the aggregate surface:

$$f_z \simeq \pi R_{ag}^2 p \tag{4}$$

We can also deduce f_z from the local stress sustained by the glassy bridge:

$$f_z \simeq \pi R_c^2 \sigma_{zz}^{loc} \quad \text{with} \quad R_c^2 \simeq R_p h_0 \tag{5}$$

where σ_{zz}^{loc} is the axial local stress within the glassy bridge and R_{ag}, R_p and R_c are the aggregate radius, the particle radius and the section size of the aforementioned glassy layer overlap,[59] respectively.
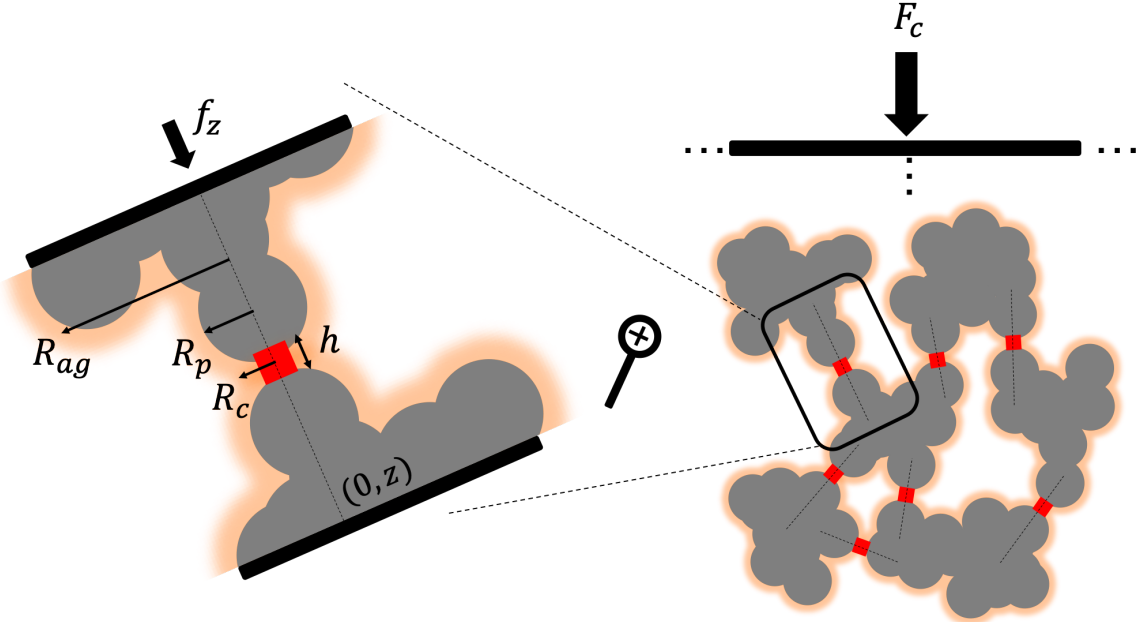

Figure 7: Schematic view of the glassy bridge network under pressure

Eqs. 4 and 5 are valid whatever the local orientation of the glassy bridge within the material. The macroscopic stress is assumed to be mainly supported by the rigid network. Thus, even if the displacement field is strictly uniaxial within the sample in a poker chip

16

geometry, it becomes triaxial due to the presence of the 3D randomly oriented particle network, as in the case of a granular system.[58]

3.4. Pressure effect on the local confinement

Assuming that the applied macroscopic pressure is carried out by the particle network, the aggregates move closer within the polymer matrix under the effect of pressure, resulting in the shortening of the glassy bridge length. The additional local confinement due to pressure leads to an increase in the local glass transition temperature in the glassy bridges that can be predicted as detailed in the following.

The glassy bridge length is assumed to depend on its initial value h_0 and on the local force felt by the aggregate f_z. Assuming a locally uniaxial compression condition, it becomes

$$h \simeq h_0 \left(1 - \frac{f_z}{\pi R_c^2 E_g} \right) \tag{6}$$

where E_g is the PDMS Young's modulus in the glassy state. Consequently, combining Eqs. 3, 4, 5 and 6, we deduce the increase in the local glass transition temperature:

$$T_g = T_g^\infty \left(1 + \frac{4\delta}{h_0} \cdot \frac{1}{1 - \frac{R_{ag}^2}{E_g R_p h_0} p} \right) \tag{7}$$

Applying the typical following values for the material parameters, we verify that the quantity $\frac{R_{ag}^2}{E_g R_p h_0} p$ is smaller than 1. We actually find $\frac{R_{ag}^2}{E_g R_p h_0} p \sim 0.08 \ll 1$, applying $R_{ag} = 50\ nm, E_g = 2\ GPa, R_p = 5\ nm, h_0 = 3\ nm$ and $p = 1\ MPa$. As a result, Eq. 7 can be simplified through a first order Taylor series expansion.

The variation in the local glass transition due to increasing of confinement with pressure is thus given by:

$$\frac{\partial T_g}{\partial p} \simeq \frac{4 T_g^\infty \delta R_{ag}^2}{E_g R_p h_0^2} \tag{8}$$

17

which is the analytical expression of the contribution due to the glassy bridge length short-ening. As illustrated in Figure 8, the pressure dependence of the local T_g is inversely pro-portional to the square of the initial length and is larger than the effect of the free volume decrease induced by pressure. For typical values of the initial bridge length ($h_0 = 3 \ nm$), Eq. 8 predicts the variation with the pressure in the local T_g of approximately 17 K/MPa, consistently with the one determined from our experiments.

To summarize, pressure changes both the free volume and the confinement degree of polymer chains in the filled rubber. These two mechanisms induce a stiffening on the me-chanical response that can be represented by a shift in the local glass transition temperature of the polymer chains connecting the neighboring particles. It clearly appears (see Figure 8) that the change in confinement due to the shortening of the glassy bridge length dominates. According to this physical picture, the pressure increases the confinement degree, leading to a significant shift in the local glass transition temperature for shorter bridges. This mech-anism seems to drive the temperature-pressure superposition law observed in real samples. However, the pressure effect strongly depends on the length of the glassy bridges that are distributed within the system. Thus, to quantitatively describe the macroscopic behavior measured on our filled elastomers, a scale-up must be performed, which is the focus of the last section.

4. A new temperature-pressure superposition law

4.1. Derivation of the temperature-pressure superposition law

Let us first recall that the pressure effect on glassy bridge mechanics is mainly reflected in a stiffening effect due to the increasing confinement induced by the shortening of the bridge length. Combining Eqs. 4, 5 and 6, the variation in the bridge length with pressure is written as
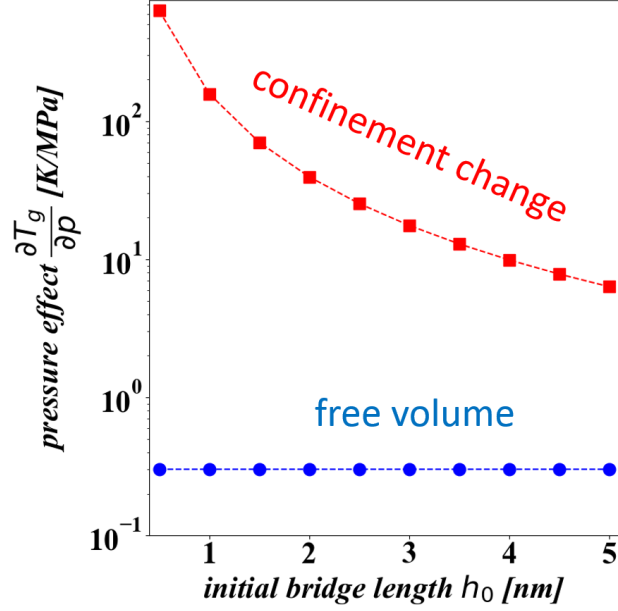
$$h(p) = h_0 - \beta p \tag{9}$$

Figure 8: Pressure effects on the local glass transition temperature of glassy bridges with respect to their initial length: $T_g^\infty = 158\ K, R_{ag} = 50\ nm, R_p = 5\ nm, \delta = 1\ nm, E_g = 2\ GPa$ and $\alpha = 0.3K/MPa$

where $\beta = \dfrac{R_{ag}^2}{R_p E_g}$. Accounting for the contribution to the confinement change, the local glass transition temperature of the glassy bridge (see Eq. 3) also depends on pressure:

$$T_g\left(z = \frac{h_0}{2}, p\right) = T_g^\infty\left(1 + \frac{4\delta}{h_0 - \beta p}\right) \tag{10}$$

Eq. 10 simply reduces to Eq. 3 at atmospheric pressure, which corresponds to the case $p = 0$ in our approach.

As discussed in the introduction, temperature has a softening effect at the macroscopic scale, which originates from the progressive loss of glassy bridges at the microscopic scale because some glassy layers no longer overlap. Therefore, temperature and pressure have antagonist effects both at the macroscopic scale and at the glassy bridge scale. Thus, different sets of specified temperatures and pressures should exist for which each of the glassy bridges of the sample exhibits the same mechanical behavior. For instance, we can search for criteria implying the glassy bridge to be in its glassy state.

19

Let us consider a bridge of initial length h_0 at $p = 0$. The polymer chains confined between the two particle surfaces behave as glassy polymers if their local glass transition temperature $T_g(z = h_0/2, p)$ (given by Eq. 10) is larger than the temperature of experiment T. On the other hand, their response is one of a rubber matrix if T is larger than $T_g(z = h_0/2, p)$. Actually, there is a switch from a rubbery response to a glassy response, as the local glass transition temperature $T_g(z = h_0/2, p)$ at the middle point of the bridge becomes larger than the temperature of experiment T. This situation occurs when the following condition is verified:

$$h_0 \leq \frac{4\delta T_g^\infty}{T - T_g^\infty} + \beta p = h^*(T, p) \tag{11}$$

We define a critical length $h^*(T, p)$ as the maximum length that a bridge should have to be in a glassy state under the experimental condition (T, p).

If we now consider another experimental condition $(T', p' = 0)$, then the same glassy bridge of initial length h_0 will behave as a glassy polymer when:

$$h_0 \leq \frac{4\delta T_g^\infty}{T' - T_g^\infty} = h^*(T', 0) \tag{12}$$

Let us discuss the physical meaning of the critical length. As discussed before, the macroscopic mechanical response of a filled rubber is driven by the particle network connected by glassy bridges. Under a given experimental condition (T, p), all polymer bridges whose lengths are shorter than the critical length $h^*(T, p)$, given by Eq. 11, are in the glassy state. Thus, if the condition $h^*(T, p) = h^*(T', 0)$ is fulfilled, then the glassy bridge network is strictly identical for the two experimental conditions. The relationship between the temperatures and pressures of the experimental conditions is given by

$$T' = T - \frac{T - T_g^\infty}{1 + \frac{4T_g^\infty}{T - T_g^\infty} \frac{\pi^*}{p}} \tag{13}$$

where $\pi^* = \dfrac{\delta}{\beta} = \dfrac{\delta R_p E_g}{R_{ag}^2}$ is a characteristic pressure whose meaning will be discussed in the next paragraph. Eq. 13 simply reduces to $T' = T$ at atmospheric pressure, which corresponds to the case $p = 0$ in our approach.

Consequently, if the two experimental conditions (T, p) and $(T', 0)$ result in the same glassy bridge network, we can also expect the macroscopic mechanical properties to be the same in that case. The shear storage modulus of the real sample $G'(T, p)$ can thus be predicted from the temperature evolution of the shear storage modulus measured at atmospheric pressure $G'(T', 0)$ as follows:

$$G'(T, p) = G'\left(T - \frac{T - T_g^\infty}{1 + \dfrac{4T_g^\infty}{T - T_g^\infty} \dfrac{\pi^*}{p}}, 0\right) \tag{14}$$

We can test this temperature-pressure superposition law on our experimental data measured on the poker chip geometry.

4.2. Discussion

According to Eq. 14, only two physical parameters T_g^∞ and π^* are involved in the temperature-pressure superposition properties of filled elastomers. The bulk glass transition temperature of the polymer matrix is easily obtained by DSC (see the experimental section). However, as we cannot measure the value of the characteristic pressure in our real sample, we kept it as an adjustable parameter for the prediction.

At a given shear strain amplitude, to predict the temperature and pressure dependence of the shear storage modulus $G'(T, p, \Delta\gamma)$, we applied the following procedure. The temperature evolution of the shear storage modulus measured at atmospheric pressure $G'(T, 0, \Delta\gamma)$ (see the black crosses in Figure 9) is fitted. This curve is used as a reference for the prediction of the temperature dependence of the modulus for a non-zero pressure (see Eq. 14). Then, we adjusted the value of the characteristic pressure π^*, that is, the single free parameter of

the problem, to obtain the best description of the experimental data for all strain amplitudes and pressures. As a result, we found $\pi^* = 2.2 \pm 0.1 \ MPa$. Figure 9 compares the temperature dependence of the shear storage modulus $G'(T, p, 4 \ \%)$ measured at iso pressure (in triangles, circles, squares and diamonds) to that predicted by our superposition law (dashed lines). A good agreement is observed between the theoretical predictions and experimental measurements on the real sample.
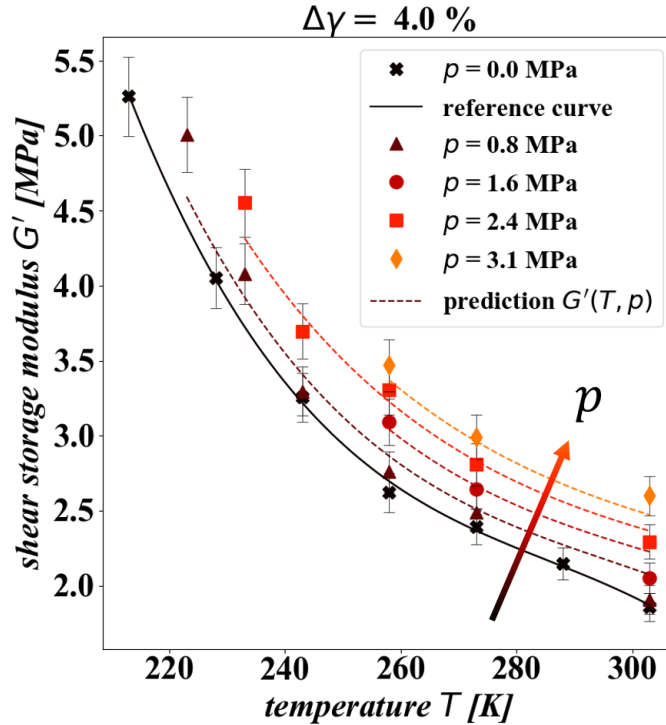

Figure 9: Shear storage modulus as a function of the temperature and pressure; comparison between theoretical predictions (dashed lines) and experimental measurements (markers) for a shear strain amplitude $\Delta\gamma = 4 \ \%$ for $T_g^\infty = 158 \ K$ and $\pi^* = 2.2 \ MPa$

The experimental values of $G'(T, p, \Delta\gamma)$ can be represented with respect to the equivalent temperature at atmospheric pressure T', which is given by Eq. 13 considering the measured bulk glass transition temperature ($T_g^\infty = 158 \ K$) and the adjusted characteristic pressure ($\pi^* = 2.2 \pm 0.1 \ MPa$). A master curve is obtained for each shear strain amplitude, as shown in Figure 10, which presents data measured at strain amplitudes of 2.4 %, 4 % and 12 %. The inset chart shows the value of the equivalent temperature at atmospheric pressure T' with respect to the experimental conditions (T, p). Only two physical parameters allow the

model to capture the pressure/temperature relative effects on the shear mechanical behavior, and to apply them in the linear and nonlinear regimes.

As a final consideration, we can estimate the value of the parameter δ that fixes the T_g gradient near the particle surface. Assuming that the aggregate radius does not vary with the strain amplitude and from the literature, $R_{ag} = 50\ nm, R_p = 5\ nm$ and $E_g = 2\ GPa$, we find a value of approximately $\delta = 0.5\ nm$, which (order of magnitude) agrees with the value reported in previous studies.[54–56] Consequently, these experimental data allow an indirect measurement of this parameter within real samples.

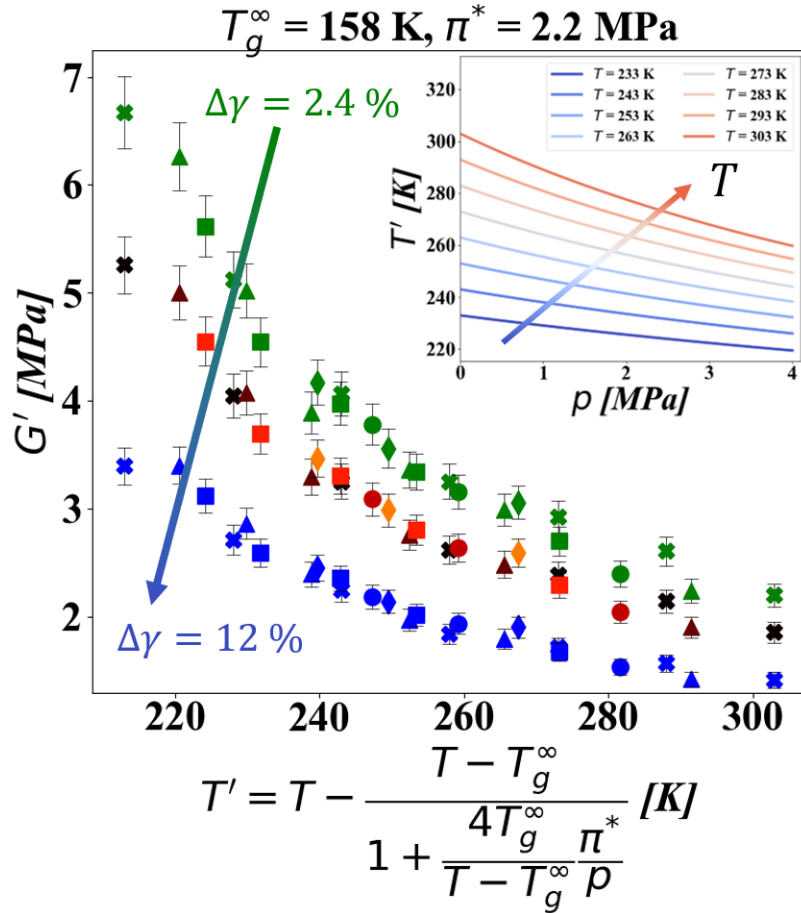

Figure 10: Master curves obtained at $\Delta\gamma = 2.4\ \%, 4\ \%$ and $12\ \%$ with $T_g^\infty = 158\ K$ and $\pi^* = 2.2\ MPa$. (inset) Equivalent temperature at atmospheric pressure T' with respect to the experimental conditions (T, p)

5. Conclusion

The addition of fillers into a polymer matrix has a major effect that goes beyond simple reinforcement, introducing unusual dependencies and nonlinearities. These specific mechanical features are commonly explained by considering a rigid network formed by fillers and the modification of its shape with the temperature and strain amplitude. According to this scenario, fillers are connected by confined polymer chains whose dynamics are slower than those in the bulk. Assuming that the dynamics of confined polymer chains can be described by the variation in their glass transition temperature with their degree of confinement, we identify the mechanism at the origin of the significant pressure effect on the mechanical response of highly filled elastomers. We show that pressure increases the degree of the confinement of polymer chains, resulting in an increase in their glass transition temperature and thus in the stiffening of their response.

In this framework, we proposed a new temperature-pressure superposition law for filled rubbers that requires only two material parameters. The first is the bulk glass transition temperature of the polymer matrix. The second is a characteristic pressure that is closely related to the structural characteristics of the filler network (particle radius, aggregate radius and range of the glass transition gradient). This new temperature-pressure superposition law accounts for experimental results measured on a silica highly filled phenylated polydimethylsiloxane (PDMS) matrix. As a result, it clearly appears that glassy bridges connecting fillers play a key role in the mechanics of the filled rubbers.

Finally, we expect the pressure effect to significantly depends on the filler concentration within the system. As a matter of fact, at lower filler concentrations, for which the interaggregate distances should be larger, we expect fewer glassy bridge connections in the filler network. In other words, we expect the pressure to induce smaller temperature shifts resulting from a larger value of the characteristic pressure π^*. In a future study, the link between the glassy bridge distribution and mechanical properties will be discussed in detail.

6. Appendix

6.1. Shear storage and loss modulus calculation: G', G''

From the single stress-strain cycles measured during the last increasing strain sweep (stage 3 in Figure 4), we deduce the shear storage modulus G' and the shear loss modulus G'' from the Fourier transform analysis of the stress and strain signals. We verify that the amplitude of the highest order components of the frequency are negligible (less than a few percent of the response) compared to the fundamental amplitude. The storage and loss moduli are thus estimated from the first harmonic of the mechanical response of our samples.

6.2. Pressure distributin within the poker chip sample: FE analysis

In triaxial fracture studies, Lindsey[39] investigated the best aspect ratio to impose a triaxial stress state in a sample that undergoes a compression force. Using an approximate analytical solution written by Schapery,[48] this author showed that the stress field is essentially triaxial above a critical aspect ratio for values of Poisson's ratio that are typical for rubber ($\nu \sim 0.5$). Moreover, the stress field along the radial position within the sample was either parabolic or flat depending on the value of the aspect ratio and Poisson's ratio. These classical results of confined amorphous polymers were also described and commented on by Creton et al.[49] in the case of thin polymer sheets.

In a previous work,[51] we showed that FE simulations (Z-set code: www.zset-software.com) can also be used to investigate the pressure distribution within the poker chip sample. We used an FE approach to better understand the characteristics of the stress field in our poker chip samples ($a = 10$) under a compression force. Using the axisymmetry of the poker chip geometry, uniaxial compression simulations are carried out by controlling the vertical displacement. In addition, to avoid volumetric locking and pressure oscillations, a three-field mixed FE formulation[50] is used on eight-node axisymmetric elements (CAX8) with a total of 9408 degrees of freedom. More details can be find in the work of Champagne et al.[51]

We computed the triaxiality ratio coming from the deviatoric and hydrostatic parts (i.e., pressure) of the stress. For a quasi-incompressible neo-Hookean material (shear modulus $G = 1\ MPa$ and bulk modulus $K_v = 2\ GPa$), we found that more than 80 % of the stress within the sample is hydrostatic (see the red part on the mesh in Figure 11). Moreover, we observed a parabolic pressure field along the radial direction ρ: its value is at the maximum at the centre of the sample ($\rho = 0$) and decreases toward zero near the outer radial limit of the sample. In other words, applying a static compression force on a quasi-incompressible matrix in the poker chip geometry used in this work is equivalent to applying a hydrostatic pressure to the sample.
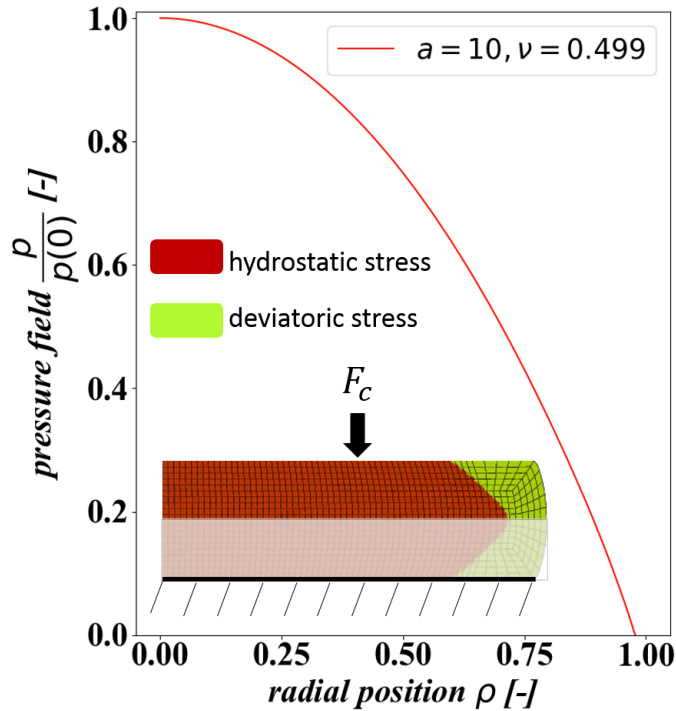

Figure 11: Numerical parabolic pressure field along the radial position ($a = 10, \nu = 0.499$)

As shown in this paper, the mechanical properties are almost linearly dependent on the static compression force (or pressure). Hence, the macroscopic mechanical response of our poker chip sample can be assumed to be the one observed at an average hydrostatic pressure p given by Eq. 2.

References

(1) Bills, K. W.; Sweeny, K. H.; Salced, F. S. The tensile properties of highly filled polymers. Effect of filler concentrations. Journal of Applied Polymer Science **1960**, 4, 259–268.

(2) Cantournet, S.; Desmorat, R.; Besson, J. Mullins effect and cyclic stress softening of filled elastomers by internal sliding and friction thermodynamics model. International Journal of Solids and Structures **2009**, 46, 2255 – 2264.

(3) Kumar, S. K.; Benicewicz, B. C.; Vaia, R. A.; Winey, K. I. 50th anniversary perspective: are polymer nanocomposites practical for applications? Macromolecules **2017**, 50, 714–731.

(4) Wang, M.-J. Effect of polymer-filler and filler-filler interactions on dynamic properties of filled vulcanizates. Rubber chemistry and technology **1998**, 71, 520–589.

(5) Mullins, L. Effect of stretching on the properties of rubber. Rubber Chemistry and Technology **1948**, 21, 281–300.

(6) Payne, A. R. The dynamic properties of carbon black-loaded natural rubber vulcanizates. Journal of applied polymer science **1962**, 6, 57–63.

(7) Kraus, G. Mechanical losses in carbon-black-filled rubbers. Journal of Applied Polymer Science: Applied Polymer Symposium **1984**, 39, 75–92.

(8) Funt, J. M. Dynamic testing and reinforcement of rubber. Rubber chemistry and technology **1988**, 61, 842–865.

(9) Huber, G.; Vilgis, T. A.; Heinrich, G. Universal properties in the dynamical deformation of filled rubbers. Journal of Physics: Condensed Matter **1996**, 8, L409.

(10) Klüppel, M.; Capella, B.; Geuss, M.; Munz, M.; Schulz, E.; Sturm, H. Filler-Reinforced Elastomers/Sanning Force Microscopy; Advances in Polymer Science; Springer Berlin Heidelberg, 2003; p 1–86.

(11) Maier, P. G.; Goritz, D. Molecular interpretation of the Payne effect. <u>Kautschuk Gummi Kunststoffe</u> **1996**, <u>49</u>, 18–21.

(12) Cheng, S.; Carroll, B.; Lu, W.; Fan, F.; Carrillo, J.-M. Y.; Martin, H.; Holt, A. P.; Kang, N.-G.; Bocharova, V.; Mays, J. W. et al. Interfacial properties of polymer nanocomposites: role of chain rigidity and dynamic heterogeneity length scale. <u>Macromolecules</u> **2017**, <u>50</u>, 2397–2406.

(13) Nguyen, H. K.; Liang, X.; Ito, M.; Nakajima, K. Direct mapping of nanoscale viscoelastic dynamics at nanofiller/polymer interfaces. <u>Macromolecules</u> **2018**, <u>51</u>, 6085–6091.

(14) Nguyen, H. K.; Sugimoto, S.; Konomi, A.; Inutsuka, M.; Kawaguchi, D.; Tanaka, K. Dynamics gradient of polymer chains near a solid interface. <u>ACS Macro Letters</u> **2019**, <u>8</u>, 1006–1011.

(15) Mujtaba, A.; Keller, M.; Ilisch, S.; Radusch, H.-J.; Beiner, M.; Thurn-Albrecht, T.; Saalwachter, K. Detection of surface-immobilized components and their role in viscoelastic reinforcement of rubber–silica nanocomposites. <u>ACS Macro Letters</u> **2014**, <u>3</u>, 481–485.

(16) Klüppel, M. Evaluation of viscoelastic master curves of filled elastomers and applications to fracture mechanics. <u>Journal of Physics: Condensed Matter</u> **2008**, <u>21</u>, 035104.

(17) Papakonstantopoulos, G. J.; Doxastakis, M.; Nealey, P. F.; Barrat, J.-L.; de Pablo, J. J. Calculation of local mechanical properties of filled polymers. <u>Physical Review E</u> **2007**, <u>75</u>, 031803.

(18) Paterson, M. S. Effect of pressure on Young's modulus and the glass transition in rubbers. <u>Journal of Applied Physics</u> **1964**, <u>35</u>, 176–179.

(19) Fillers, R. W.; Tschoegl, N. W. The effect of pressure on the mechanical properties of polymers. <u>Transactions of the Society of Rheology</u> **1977**, <u>21</u>, 51–100.

(20) Cheng, Z.-Y.; Gross, S.; Zhang, Q. M. Pressure-temperature study of dielectric relaxation of a polyurethane elastomer. Journal of Polymer Science **1999**, 37, 983–990.

(21) Alkhader, M.; Knauss, W. G.; Ravichandran, G. A new shear-compression test for determining the pressure influence on the shear response of elastomers. Experimental Mechanics **2012**, 52, 1151–1161.

(22) Ferry, J. D.; Stratton, R. A. The free volume interpretation of the dependence of viscosities and viscoelastic relaxation times on concentration, pressure, and tensile strain. Kolloid-Zeitschrift **1960**, 171, 107–111.

(23) Merabia, S.; Long, D. Heterogeneous Dynamics and Pressure Dependence of the Dynamics in van der Waals Liquids. Macromolecules **2008**, 41, 3284–3296.

(24) Quach, A.; Simha, R. Pressure-volume-temperature properties and transitions of amorphous polymers; polystyrene and poly (orthomethylstyrene). Journal of Applied Physics **1971**, 42, 4592–4606.

(25) Zoller, P. A study of the pressure-volume-temperature relationships of four related amorphous polymers: polycarbonate, polyarylate, phenoxy, and polysulfone. Journal of Polymer Science: Polymer Physics Edition **1982**, 20, 1453–1464.

(26) Rodgers, P. A. Pressure–volume–temperature relationships for polymeric liquids: a review of equations of state and their characteristic parameters for 56 polymers. Journal of Applied Polymer Science **1993**, 48, 1061–1080.

(27) Walsh, D.; Zoller, P. Standard pressure volume temperature data for polymers; CRC Press, 1995.

(28) Vogt, B. D. Mechanical and viscoelastic properties of confined amorphous polymers. Journal of Polymer Science Part B: Polymer Physics **2018**, 56, 9–30.

(29) Keddie, J. L.; Jones, R. A.; Cory, R. A. Size-dependent depression of the glass transition temperature in polymer films. EPL (Europhysics Letters) **1994**, <u>27</u>, 59.

(30) Forrest, J. A.; Dalnoki-Veress, K.; Dutcher, J. R. Interface and chain confinement effects on the glass transition temperature of thin polymer films. Physical Review E **1997**, <u>56</u>, 5705.

(31) Fukao, K.; Miyamoto, Y. Glass transitions and dynamics in thin polymer films: dielectric relaxation of thin films of polystyrene. Physical Review E **2000**, <u>61</u>, 1743.

(32) Grohens, Y.; Brogly, M.; Labbe, C.; David, M.-O.; Schultz, J. Glass transition of stereoregular poly (methyl methacrylate) at interfaces. Langmuir **1998**, <u>14</u>, 2929–2932.

(33) Berriot, J.; Lequeux, F.; Monnerie, L.; Montes, H.; Long, D.; Sotta, P. Filler–elastomer interaction in model filled rubbers, a 1H NMR study. Journal of Non-Crystalline Solids **2002**, <u>307</u>, 719–724.

(34) Berriot, J.; Montes, H.; Lequeux, F.; Long, D.; Sotta, P. Evidence for the shift of the glass transition near the particles in silica-filled elastomers. Macromolecules **2002**, <u>35</u>, 9756–9762.

(35) Colombo, D.; Montes, H.; Lequeux, F.; Cantournet, S. Thermo-mechanical modeling of a filled elastomer based on the physics of mobility reduction. Mechanics of Materials **2020**, 103319.

(36) Merabia, S.; Sotta, P.; Long, D. R. A microscopic model for the reinforcement and the nonlinear behavior of filled elastomers and thermoplastic elastomers (Payne and Mullins effects). Macromolecules **2008**, <u>41</u>, 8252–8266.

(37) Froltsov, V. A.; Klüppel, M.; Raos, G. Molecular dynamics simulation of rupture in glassy polymer bridges within filler aggregates. Physical Review E **2012**, <u>86</u>, 041801.

(38) Sodhani, D.; Reese, S. Finite element-based micromechanical modeling of microstructure morphology in filler-reinforced elastomer. Macromolecules **2014**, 47, 3161–3169.

(39) Lindsey, G. H. Triaxial fracture studies. Journal of Applied Physics **1967**, 38, 4843–4852.

(40) Kakavas, P. A.; Blatz, P. J. Effects of voids on the response of a rubber poker chip sample. Journal of Applied Polymer Science **1991**,

(41) Motamed, A.; Bhasin, A.; Liechti, K. M. Using the poker-chip test for determining the bulk modulus of asphalt binders. Mechanics of Time-Dependent Materials **2014**, 18, 197–215.

(42) Ovalle Rodas, C.; Zaïri, F.; Naït-Abdelaziz, M. A finite strain thermo-viscoelastic constitutive model to describe the self-heating in elastomeric materials during low-cycle fatigue. Journal of the Mechanics and Physics of Solids **2014**, 64, 396–410.

(43) Chazeau, L.; Brown, J. D.; Yanyo, L. C.; Sternstein, S. S. Modulus recovery kinetics and other insights into the Payne effect for filled elastomers. Polymer composites **2000**, 21, 202–222.

(44) Reynolds, O. On the Theory of Lubrication and Its Application to Mr. Beauchamp Tower's Experiments, Including an Experimental Determination of the Viscosity of Olive Oil. Philosophical Transactions of the Royal Society of London (1776-1886) **1886**, 177, 157–234.

(45) Gent, A. N.; Lindley, P. B. The Compression of Bonded Rubber Blocks. Proceedings of the Institution of Mechanical Engineers **1959**, 173, 111–122.

(46) Gent, A. N.; Lindley, P. B. Internal rupture of bonded rubber cylinders in tension. The Royal Society **1959**, 249, 195–205.

(47) Gent, A. N.; Meinecke, E. A. Compression, bending, and shear of bonded rubber blocks. Polymer Engineering & Science **1970**, 10, 48–53.

(48) Lindsey, G. H.; Schapery, R. A.; Williams, M. L.; Zak, A. R. The triaxial tension failure of viscoelastic materials. Aeronautical Reseach Laboratory ARL **1963**,

(49) Creton, C.; Lakrout, H. Micromechanics of flat-probe adhesion tests of soft viscoelastic polymer films. Journal of Polymer Science Part B: Polymer Physics **2000**, 38, 965–979.

(50) Al Akhrass, D.; Bruchon, J.; Drapier, S.; Fayolle, S. Integrating a logarithmic-strain based hyperelastic formulation into a three-field mixed finite element formulation to deal with incompressibility in finite-strain elastoplasticity. Finite Elements in Analysis and Design **2014**, 86, 61–70.

(51) Champagne, J.; Ovalle, C.; Cantournet, S.; Lequeux, F.; Montes, H.; Le-Gorju, K. Hydrostatic pressure effect on the non-linear mechanics of filled rubbers: experiments and physico-mechanical approach. Constitutive Models for Rubbers XI. Nantes, France, 2019; pp 194–199.

(52) Long, D.; Lequeux, F. Heterogeneous dynamics at the glass transition in van der Waals liquids, in the bulk and in thin films. The European Physical Journal E **2001**, 4, 371–387.

(53) Mattsson, J.; Forrest, J. A.; Börjesson, L. Quantifying glass transition behavior in ultrathin free-standing polymer films. Physical Review E **2000**, 62, 5187.

(54) Montes, H.; Lequeux, F.; Berriot, J. Influence of the glass transition temperature gradient on the nonlinear viscoelastic behavior in reinforced elastomers. Macromolecules **2003**, 36, 8107–8118.

(55) Gradmann, S.; Medick, P.; Rossler, E. A. Glassy dynamics in nanoconfinement as revealed by ^{31}P NMR. The Journal of Physical Chemistry B **2009**, 113, 8443–8445.

(56) Papon, A.; Montes, H.; Hanafi, M.; Lequeux, F.; Guy, L.; Saalwächter, K. Glass-transition temperature gradient in nanocomposites: evidence from nuclear magnetic resonance and differential scanning calorimetry. Physical review letters **2012**, _108_, 065702.

(57) Cho, K.; Gent, A. Cavitation in model elastomeric composites. Journal of Materials Science **1988**, _23_, 141–144.

(58) Radjai, F.; Wolf, D. E.; Jean, M.; Moreau, J.-J. Bimodal character of stress transmission in granular packings. Physical review letters **1998**, _80_, 61.

(59) Colombo, D. Modeling the macroscopic mechanical behavior of filled elastomers from local polymer dynamics. Ph.D. thesis, MinesParistech, 2016.

Graphical TOC Entry

Some journals require a graphical entry for the Table of Contents. This should be laid out "print ready" so that the sizing of the text is correct. Inside the `tocentry` environment, the font used is Helvetica 8 pt, as required by Journal of the American Chemical Society.

The surrounding frame is 9 cm by 3.5 cm, which is the maximum permitted for Journal of the American Chemical Society graphical table of content entries. The box will not resize if the content is too big: instead it will overflow the edge of the box.

This box and the associated title will always be printed on a separate page at the end of the document.